Multistep Redoxsystems, LX[1]

1,4,5,8-Tetraoxo-1,4,5,8-tetrahydrothianthrene: Synthesis, Structure, and Spectroelectrochemical Properties

Siegfried Hünig*[a], Klaus Sinzger[a], Robert Bau*[b], Tobias Metzenthin[b], and Josef Salbeck*[c]

Institut für Organische Chemie der Universität Würzburg[a], Am Hubland, W-8700 Würzburg

Chemistry Department, University of Southern California[b], Los Angeles, CA 90089, USA

Institut für Organische Chemie der Universität Regensburg[c], Universitätsstraße 31, W-8400 Regensburg

Received July 20, 1992

Key Words: Thianthrene derivatives / X-ray analysis / MO calculation / Cyclovoltammetry / UV-Vis spectroelectrochemistry

The synthesis, structure, cyclovoltammetric and spectroelectrochemical data of 1,4,5,8-tetraoxo-1,4,5,8-tetrahydrothianthrene (**2a**) are presented. A relation between the positive partial charge at the sulfur atom and the dihedral angle at the S–S axis is discussed on the basis of semiempirical MO calculations.

Recently, the well-known class of thianthrenes has gained new interest in the field of redox chemistry[2]. Thianthrenes with electron-releasing substituents (i.e. **1b**[3]) as donors and the quinoid 1,4,5,8-tetraoxo-1,4,5,8-tetrahydrothianthrenes **2** [in the following called thianthrenediquinones (TDQ)] as acceptors represent promising precursors of electrically conducting materials.

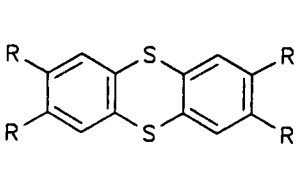

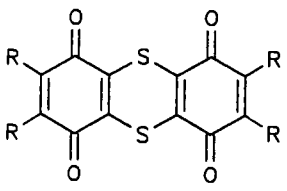

1a, R=H; **1b**, R=OCH_3 **2a**, R=H; **2b**, R=CH_3; **2c**, R=

Since planarity of the participating π systems is an essential precondition for electrical conductivity[4], the structures of **1b** and **2** are of special interest. While neutral **1b**, analogous to the unsubstituted compound **1a**, is folded along the S–S axis in a roof-like manner[5], there is a planar radical cation in solid [**1b**][$SbCl_6$][6].

In the course of our work on quinoid acceptors, particularly on *N,N'*-dicyanoquinone diimines (DCNQIs)[7], we were also interested in the thianthrenediquinones **2**, especially in the interrelation between their redox properties and their structures. Quite recently, the structure of a thianthrenediquinone derivative **2c** was reported for the first time[8]. As described, compound **2c** is completely planar in the solid state.

While the tetramethyl derivative **2b**[9] and the dibenzo derivative **2c**[10] are known for a long time, attempts to synthesize the unsubstituted compound **2a** – analogous to the synthesis of **2b** and **2c** – from 2,3-dichloro-*p*-benzoquinone and sodium sulfide or hydrogen sulfide failed[9]. In the following, we report on the synthesis and structure, as well as the redox and spectroelectrochemical properties of the unsubstituted thianthrenediquinone derivative **2a**.

Synthesis of Thianthrenediquinone 2a

The synthesis of **2a** was achieved by means of Diels-Alder protective-group strategy according to a reaction sequence for the synthesis of 2,3-bis(alkylthio)-*p*-benzoquinones published by Wladislaw et al.[11] (Scheme 1).

Scheme 1. R.T. = room temperature

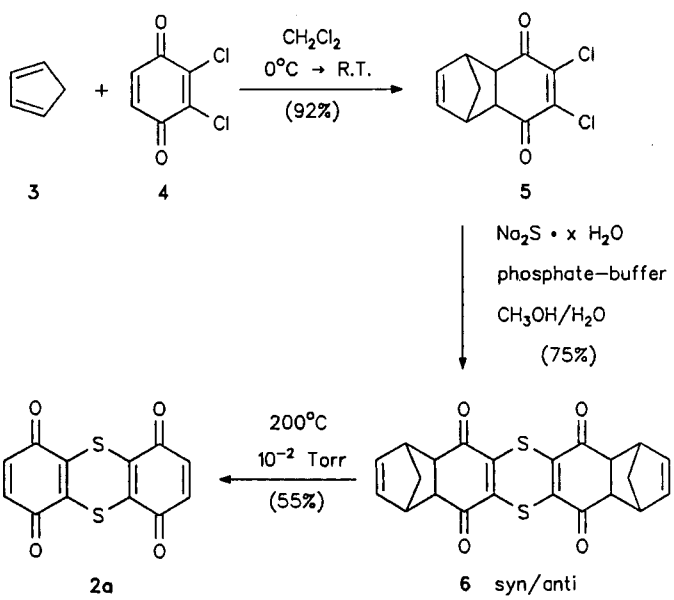

  0009–2940/93/0202–0465 $ 3.50+.25/0

As starting compound, the known Diels-Alder adduct **5**[12], obtained from 2,3-dichloro-*p*-benzoquione (**4**) and cyclopentadiene (**3**), was used. The yield of **5** (74%[12]) could be increased up to 92% by applying 1.5 equivalents of cyclopentadiene in dichloromethane. After reaction of **5** with sodium sulfide in methanol/water in the presence of a phosphate buffer (pH 7), we obtained compound **6** in 75% yield. A buffer was necessary to avoid tautomerization of enediones **5** and **6**. Vacuum thermolysis of **6** resulted in 55% yield of compound **2a**. Analogous to the substituted derivatives **2b** and **2c**, the deeply violet **2a** shows only a slight solubility in common organic solvents at room temperature, but quite good solubility in acetic acid, chlorobenzene, and other higher boiling chlorinated hydrocarbons, when heated.

Crystal Structure of 2a

The unit cell consists of 16 molecules of **2a** forming four equivalent groups, each consisting of four crystallographically independent molecules. Three molecules of such a group (labeled molecules **2a'**, **2a''** and **2a'''** in Figure 1) are bisected by a mirror plane passing through their S–S axes. The fourth molecule (see molecule **2a** in Figure 1) is rotated by 90° compared to the other three molecules, and it is bisected along its lateral axis. This fourth molecule separates two nearly perpendicularly arranged triple stacks, as shown in Figure 2b. Moreover, its molecular plane is parallel to the molecular planes of one stack, and is also parallel to the stacking axis of the other stack. As a result, **2a** reveals a much higher crystal symmetry than **2c**, which contains only one molecule per unit cell.

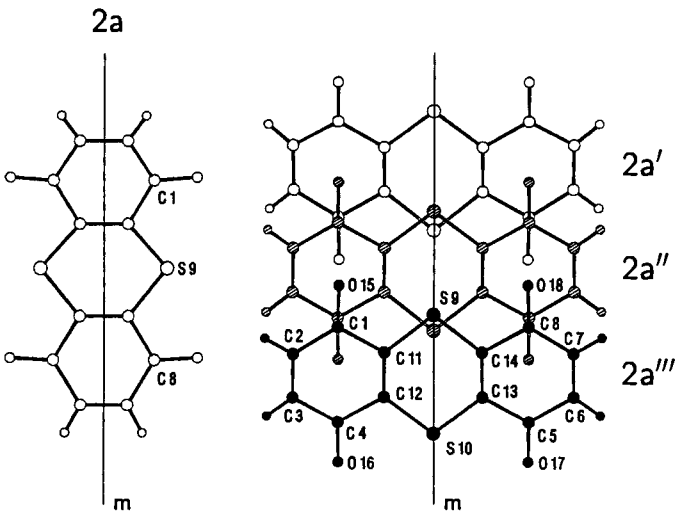

Figure 1. Numbering scheme for the atoms of **2a**

In the crystal of **2c** there is a uniform stacking of the molecules with an interplanar distance of 345 pm[8], while in the crystal of **2a** the molecules are arranged in a triple stack with interplanar distances of 338 and 347 pm, respectively, and a transversal shift of the molecule planes by 159 and 170 pm, respectively (Figure 3). **2c** additionally reveals a shift in lateral direction (Figure 3). As the authors argue[8],

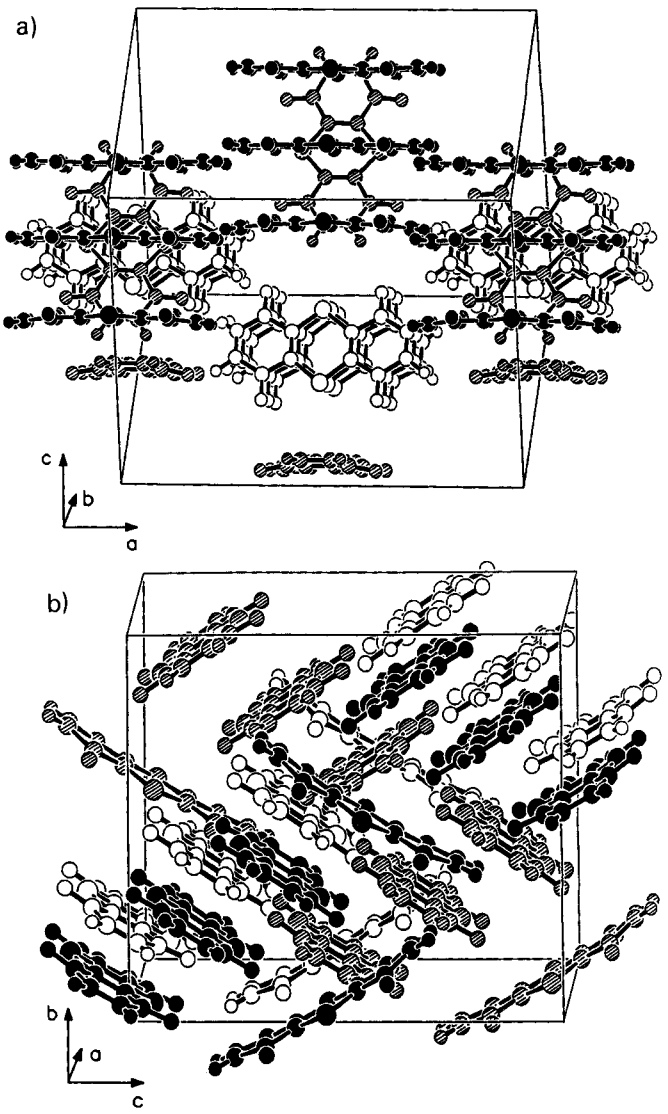

Figure 2. Two views on the unit cell of **2a**. Black atoms are towards the reader, white atoms are away from the reader and shaded atoms are intermediate (SCHAKAL 88B/V16)

this stacking mode is due to an optimal overlap of HOMOs and LUMOs. Actually, in terms of orbital symmetry, there is a "ring over bond"-like arrangement, allowing at least to some extent binding HOMO-LUMO interactions in **2c** (Figure 3). On the contrary, the stacking mode of **2a** prevents an effective HOMO-LUMO overlap (Figure 3). Therefore, the different stacking modes of **2a** and **2c** are more likely due to packing effects in the crystal.

In the crystal, **2a** is nearly planar, as is **2c**. Only the C=O groups stick out of the molecule plane by 2–10°. Presumably, this is due to a repulsion of the sulfur and oxygen lone pairs. Interestingly, semiempirical calculations[14] also predicted structures with C=O groups sticking out of the plane of the quinoid ring (AM1: about 18°; MNDO: about 25°). The bond lengths and angles of **2a** (Tables 1 and 2), especially the C–S distances (174.8–176.5 pm) and C–S–C angles (100.7–102.0°), are in good agreement with those reported for **2c**[8].

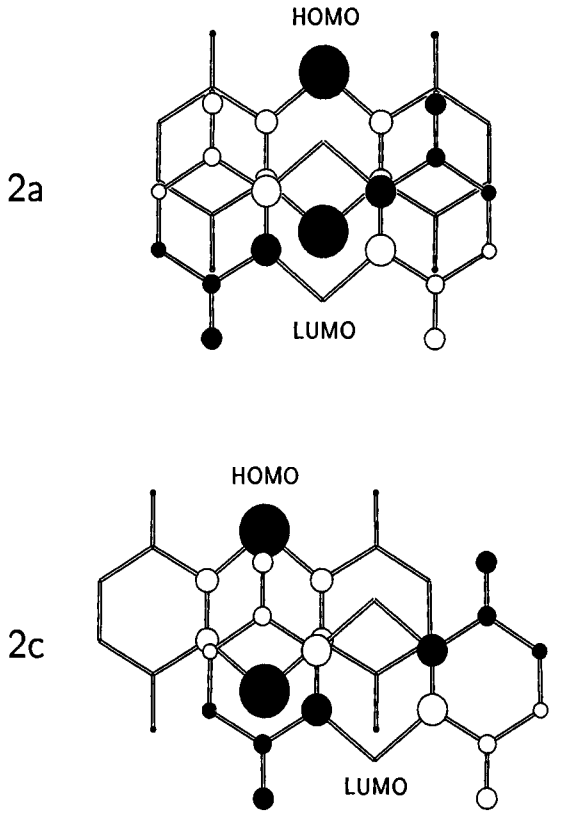

Figure 3. Overlapping of frontier orbitals (HOMO and LUMO) for two neighboring molecules of **2a** (above) and **2c** (below; only the thianthrene core is drawn) in the crystal. Coefficients are obtained on the basis of AM1 calculations. (Those obtained from MNDO calculations, cf. ref.[8], are quite similar)

Table 1. Bond lengths [pm] of **2a**

Molecule **2a**			
C1-C2	147.1(9)	C8-C7	147.1(11)
C2-C3	135.5(14)	C7-C6	132.9(17)
C3-C4	147.1(9)	C6-C5	147.1(11)
C4-C12	148.5(8)	C5-C13	148.8(10)
C12-C11	135.6(11)	C13-C14	135.2(13)
C11-C1	148.5(8)	C14-C8	148.8(10)
C11-S9	174.8(6)	C14-S9	174.9(7)
C12-S10	174.8(6)	C13-S10	174.9(7)
C1-O15	121.6(8)	C8-O18	121.6(9)
C4-O16	121.6 (8)	C5-O17	121.6(9)
Molecule	**2a'**	**2a''**	**2a'''**
C1-C2	147.9(9)	146.6(10)	146.9(10)
C2-C3	132.9(11)	132.3(11)	130.1(12)
C3-C4	145.7(9)	146.3(10)	146.9(11)
C4-C12	149.1(8)	148.5(9)	148.8(9)
C12-C11	132.6(9)	132.8(8)	133.7(9)
C11-C1	149.1(8)	149.3(9)	149.6(9)
C11-S9	176.1(6)	176.2(7)	175.7(7)
C12-S10	176.5(6)	176.5(7)	175.6(7)
C1-O15	121.1(8)	120.9(9)	120.4(9)
C4-O16	121.5(8)	121.6(8)	121.8(10)

To explain the planarity of $\mathbf{1b}^{\bullet+}$ and **2c**, the authors mentioned the presence of mesomeric stabilization due to participation of the sulfur[6,8]. This assumption was supported by MNDO calculations on **1b** and $\mathbf{1b}^{\bullet+}$[2a]. For $\mathbf{1b}^{\bullet+}$,

Table 2. Bond angles [°] of **2a**

Molecule **2a**			
C1-C2-C3	120.3(7)	C8-C7-C6	121.1(7)
C2-C3-C4	120.3(7)	C7-C6-C5	121.1(7)
C3-C4-C12	119.1(6)	C6-C5-C13	118.3(7)
C4-C12-C11	119.9(6)	C5-C13-C14	120.2(6)
C12-C11-C1	119.9(6)	C13-C14-C8	120.2(6)
C11-C1-C2	119.1(6)	C14-C8-C7	118.3(7)
C1-C11-S9	111.1(4)	C8-C14-S9	110.9(5)
C11-S9-C14	102.0(3)	–	–
C12-C11-S9	128.9(5)	C13-C14-S9	128.9(5)
C4-C12-S10	111.1(4)	C5-C13-S10	110.9(5)
C12-S10-C13	102.0(3)	–	–
C11-C12-S10	128.9(5)	C14-C13-S10	128.9(5)
O15-C1-C2	121.1(6)	O18-C8-C7	121.9(7)
O15-C1-C11	119.9(6)	O18-C8-C14	119.8(8)
O16-C4-C3	121.1(6)	O17-C5-C6	121.9(7)
O16-C4-C12	119.9(6)	O17-C5-C13	119.8(8)
Molecule	**2a'**	**2a''**	**2a'''**
C1-C2-C3	120.5(6)	122.4(7)	122.2(7)
C2-C3-C4	121.7(6)	119.6(7)	121.4(7)
C3-C4-C12	118.1(6)	119.4(6)	118.2(7)
C4-C12-C11	120.5(5)	120.4(6)	120.2(6)
C12-C11-C1	120.7(5)	120.3(6)	120.6(6)
C11-C1-C2	117.8(6)	117.8(6)	117.3(6)
C1-C11-S9	110.1(5)	110.3(5)	110.1(5)
C11-S9-C14	101.3(3)	101.4(3)	101.1(3)
C12-C11-S9	129.1(5)	129.4(5)	129.5(5)
C4-C12-S10	109.8(4)	110.4(5)	110.6(5)
C12-S10-C13	100.7(3)	101.4(3)	101.4(3)
C11-C12-S10	129.6(5)	129.2(5)	129.2(5)
O15-C1-C2	121.8(6)	122.5(7)	123.1(7)
O15-C1-C11	120.4(6)	119.7(7)	119.6(6)
O16-C4-C3	122.5(6)	120.8(6)	122.2(7)
O16-C4-C12	119.4(5)	119.7(6)	119.5(7)

a planar structure with a distinctly higher positive partial charge on the sulfur ($\delta_S = +0.50$) as compared to **1b** ($\delta_S = +0.25$) was calculated. We were able to verify these results with minor deviations and, additionally, we obtained a qualitatively similar result by AM1 calculations (Table 3). The resonating structures, which best reflect the results obtained from the calculations, are drawn in Scheme 2.

Scheme 2

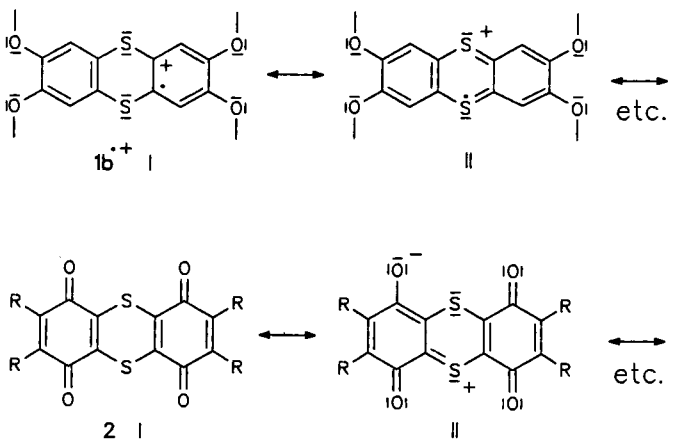

From this, the question arose whether a correlation could be derived between the calculated partial charges at the sulfur and the calculated or observed dihedral angles at the S–S axis. To test the reliability of such calculations, we performed them with different methods on differently substituted thianthrene and dithiine derivatives (**1**, **2a**, **7**, **8**) with known crystal structures.

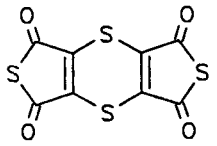

7

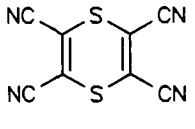

8

Table 3. Comparison of dihedral angles φ, obtained by different computational methods and from crystal data, respectively, with calculated partial charges δ_S at the sulfur atoms and δ_O at the oxygen atoms for thianthrene derivatives **1a**, **1b**, **2a**, and dithiine derivatives **7**, **8**

	PCMODEL		AM1			MNDO			Crystal	
	φ [°]	φ [°]	δ_S	δ_O	φ [°]	δ_S	δ_O	φ [°]	Lit.
1a	125	169	0.38	–	155	0.25	–	128	[16]
1b	125	160	0.38	–0.18	153[a]	0.25	– 0.27	131	[5]
1b$^{\bullet+}$	–	180	0.75	–0.16	180[b]	0.47	–0.24	180	[6]
2a	123	179	0.53	–0.24	167	0.35	–0.24	180	[c]
2a$^{\bullet-}$	–	169	0.54	–0.35	149	0.32	–0.35	–	–
2a^{2-}	–	179	0.55	–0.47	154	0.30	–0.46	–	–
7	130	180	0.61	–0.19	180	0.42	–0.19	180	[17]
8	129	180	0.51	–	180	0.33	–	124	[18]

[a] Ref.[2a]: φ = 150°, δ_S = 0.25, δ_O = –0.27. – [b] Ref.[2a]: φ = 180°, δ_S = 0.50, δ_O = –0.25. – [c] This work.

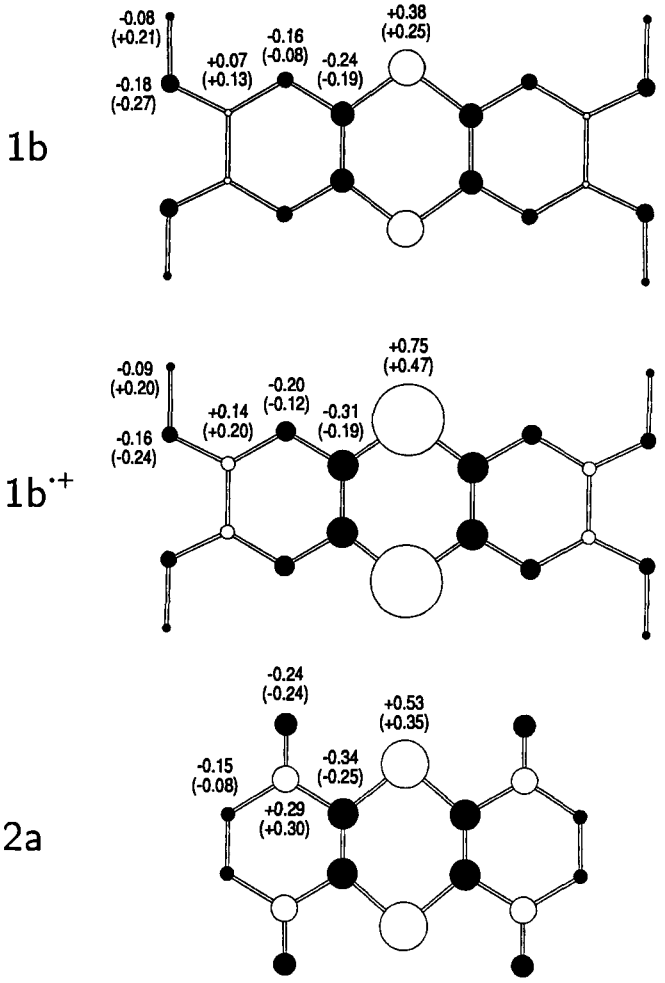

Figure 4. Charge distribution of **1b**, **1b**$^{\bullet+}$, and **2a** obtained from AM1 (MNDO) calculations (cf. Table 3)

As expected, PCMODEL (MMX)[15], a pure force-field method often used for preoptimization, which neglects π interactions, computes dihedral angles between 123 and 130° for all molecules in Table 3, which are all in the range of the dihedral angle of the unsubstituted thianthrene **1a** found in the crystal (φ = 128°). The semiempirical methods AM1 and MNDO, both including π interactions, calculate the same qualitative sequence concerning the partial charge at the sulfur, with distinctly higher positive values by the AM1-method (Table 3). Although no definite correlation can be derived, as a trend one can notice that a higher positive charge (δ_S) at the sulfur atom, corresponding to an increasing contribution of the resonating structures **II** (Scheme 2), results in increasing (calculated) dihedral angles φ along the S–S axis. For **2a**, both methods (AM1 and MNDO) calculate partial charges at the sulfur atom intermediate between **1b** and **1b**$^{\bullet+}$ (Figure 4).

However, the dihedral angles calculated for **2a** (AM1: 179°; MNDO: 167°), at least the MNDO result, differ somewhat from that found in the crystal (180°). Presumably, this deviation is due to the above mentioned repulsion of the lone pairs of the sulfur and oxygen atoms. Compared to this result, for compound **7** (isoelectronic to **2a**) with C=O groups involved in a five-membered ring and, therefore, more remote from the sulfur atoms, both methods calculate absolutely planar structures (including the C=O groups) as found in the crystal[17]. It should be noted here that both AM1 and MNDO, in contrast to the distinct differences concerning the sulfur, compute nearly the same negative partial charges (δ_O) at the oxygen atoms for each **2a**, **2a**$^{\bullet-}$, **2a**$^{2-}$, and **7**. For complete planarity of **2a**, a barrier of 1.1 kJ/mol (AM1) and 5.2 kJ/mol (MNDO) is calculated. Therefore, the nearly planar structure of **2a** in the crystal is probably due to packing effects[2a]. For the anions **2a**$^{\bullet-}$ and **2a**$^{2-}$ AM1 and MNDO reveal somewhat diverging results. While AM1 calculates nearly planar structures for **2a**$^{\bullet-}$ (with φ = 169° somewhat more apart from 180°) and **2a**$^{2-}$ (φ = 179°) with the partial charge at the sulfur weakly increasing (δ_S: +0.53 → +0.55), MNDO computes structures with striking deviations from planarity (**2a**$^{\bullet-}$: φ = 149°; **2a**$^{2-}$: φ = 154°) and with δ_S weakly decreasing (+0.35 → +0.31). On the other hand, for both **2a**$^{\bullet-}$ and **2a**$^{2-}$ a diminished energetic barrier to complete planarization (**2a**$^{\bullet-}$: ≈3 kJ/mol; **2a**$^{2-}$: ≈1.5 kJ/mol) as compared to **2a** (≈5 kJ/mol) is calculated by MNDO. The dihedral angles calculated for the aromatic thianthrene derivatives **1a** and **1b** differ strongly upwards from those found in the crystal (cf. ref.[2a],

indicating an overestimated π-bonding contribution of the sulfur. The most striking deviation between calculated (180°) and observed (124°) dihedral angle, however, is found for the dithiine derivative **8**. In this context, a general problem of comparing calculated and crystal structures should be taken into account: While calculations treat isolated molecules (in the ideal vapor phase), intermolecular interactions and packing effects play an important part in the crystal (condensed phase). Therefore, and with regard to its potential suitability as a component in conducting materials, a thorough examination of **2a** in solution, especially of its reduced redox states, seemed to be of great interest.

Electrochemical Behavior of 2a

Cyclovoltammetric measurements on **2a** in acetonitrile reveal two reversible halfwave potentials at −0.01 and −0.33 V. The formation of the trianion and the tetraanion appears unresolved as a single quasi-reversible signal at −1.56 V. For the three diquinones **2a**, **10**, **11a**, a comparison of the potential differences between the formation of the radical anion and the formation of the dianion admits predictions about the interaction of the quinoid moieties. Thereby, **2a** (320 mV in acetonitrile; 360 mV extrapolated for DMF) occupies an intermediate position between the angled triptycenediquinone **10** (175 mV in acetonitrile; 230 mV in DMF), whose quinoid moieties are linked by sp^3-hybridized carbons, and the planar anthracenediquinone **11a** (480 mV in DMF), whose moieties are connected by sp^2-hybridized carbon atoms (Table 4).

Besides, a comparison of the absorption bands of the radical anions in the UV/Vis spectra is very instructive. Thus, one can find again the absorptions of the radical anion of unsubstituted benzoquinone (421, 446 nm) for each of the compounds **2a**, **10**, **11a** as well as **9**. Moreover, the radical anions of the three compounds **2a**, **10**, and **11a**, in contrast to those of the unsubstituted benzoquinone and compound **9**, reveal further signals in the NIR region. **10** shows a weak absorption at 1200 nm with ε = 160, **2a** likewise a very broad signal at 1500 nm with ε = 1780, whereas **11a**, besides a band at 1286 nm, shows a relatively narrow and intensive signal at 1560 nm with ε = 16000.

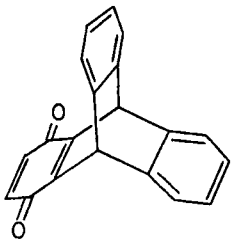

9

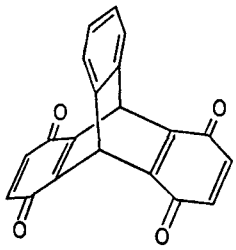

10

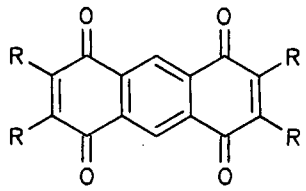

11a, R=H; **11b**, R=CH_3; **11c**, R=

As a result, the values of **2a** obtained both from electrochemical as well as spectroelectrochemical measurements are intermediate between those of **10**, which is described as a localized radical anion as a result of ESR measurements[20], and **11a**, which is reported to be delocalized[19]. According to a simplified theory of Hush[21], the intensity of the observed NIR absorption band is proportional to the square of the electronic coupling between both quinoid moieties. Hence, in **2a** there is a distinct interaction of the quinoid

Table 4. Cyclovoltammetric and spectroelectrochemical data of diquinones **2**, **10**, **11**, and monoquinone **9**

CV	CH_2Cl_2 [a]			CH_3CN [b]			DMF [c]		
	$E^1_{1/2}$ [mV]	$E^2_{1/2}$ [mV]	ΔE [mV]	$E^1_{1/2}$ [mV]	$E^2_{1/2}$ [mV]	ΔE [mV]	$E^1_{1/2}$ [mV]	$E^2_{1/2}$ [mV]	ΔE [mV]
2a	± 0	−300	300	−10	−330	320	–	–	~360[d]
2b	−180	−500	320	−165	−500	335	−180	−560	380
2c	−130	−460	330	−140	−480	340	−170	−550	380
9	–	–	–	−305	−1105	800	–	–	–
10	–	–	–	−240	−415	175	−240	−470	230
11a	–	–	–	–	–	–	−260	−740	480
11b	–	–	–	–	–	–	−410	−890	480
11c	–	–	–	–	–	–	−420	−920	500

UV/VIS	Monoanion λ[nm]	Dianion λ[nm]	Tetraanion λ[nm]
2a[e]	421, 448, **1500**	408, 433, 506, **865**	390
9[e]	423, 442	380	–
10[e]	420, 442, **1200**	420, 442, 514	350
11a[f]	410, 440, **1286**, **1560**	**866**	no information

[a] Vs. Ag/AgCl, $TBABF_4$, this work. – [b] Vs. Ag/AgCl, $TBAPF_6$, this work. – [c] **2b**, **2c**: vs. SCE, $TBAClO_4$, from ref.[2b]. – **8**, **9a–c**: vs. SCE, $TBABF_4$, from ref.[19]. – [d] Evaluated. – [e] In CH_3CN, this work. – [f] In DMF; from ref.[19].

moieties mediated by the sulfur bridges. The weaker electronic coupling of **10**, which results in a NIR absorption of only $\varepsilon = 160$, nevertheless leads to a shift of the first reduction potential by 65 mV to more positive values compared to **9**, which is due to through-space Coulomb interactions.

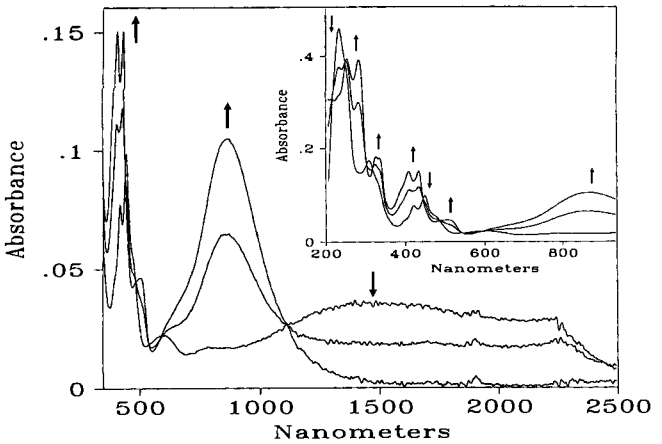

Figure 5. Spectroelectrochemistry during the reduction of radical anion $\mathbf{2a}^{\bullet -}$ to the dianion, $c = 1.3$ mM in acetonitrile, 0.1 M TBAHFP. Inset: UV/Vis part

Besides a new weak signal at 514 nm and vanishing of the NIR absorption at 1200 nm, reduction of triptycenediquinone **10** to the dianion results only in a doubled extinction of the shorter-wave signals at 420 and 442 nm. This is in agreement with a bis-radical anion structure[20] and again reflects the weak coupling of both quinoid moieties in this molecule. On the other hand, **2a** reveals a distinct shift of the signals, and, most strikingly, it shows a new signal at 865 nm. This shift of the absorption signals indicates again a stronger interaction of the quinoid moieties in **2a**. Moreover, the NIR absorption at 865 nm is in excellent agreement with the dianion absorption of anthracenediquinone **11a** at 866 nm[19]. For each, **10** and **2a**, further reduction to the tetraanion results in a new band at 350 and 390 nm, respectively. Concerning position and structure of the bands, these absorptions are comparable to that of the benzoquinone dianion at 367 nm under the same conditions.

CT Complex of 2a with TMTTF

Reaction of **2a** with TMTTF in acetonitrile yields a 1:1 CT complex (tiny black needles), which shows a powder conductivity of $< 10^{-7}$ Scm^{-1} at room temperature, indicating the presence of a "mixed-stack" complex. Further investigations, i.e. structure determination of the CT complex, are in progress.

This work was supported by the *Fonds der Chemischen Industrie*. T. M. thanks the *Deutsche Forschungsgemeinschaft* for a research grant.

Experimental

1,4,5,8-Tetraoxo-1,4,5,8-tetrahydrothianthrene (**2a**): 19.4 g (80.0 mmol) of **5**[12], available by the reaction of 2,3-dichloro-*p*-benzoquinone (**4**) with 1.5 equivalents of cyclopentadiene (**3**) in dichloromethane at room temp. (36 h; 92% yield) is suspended in a buffer solution (pH 7) of 6.24 g (40.0 mmol) of $NaH_2PO_4 \cdot 2\ H_2O$ and 1.42 g (10.0 mmol) of Na_2HPO_4 in 100 ml of water/methanol (1:1). A solution of 18.7 g (84.0 mmol) of $Na_2S \cdot H_2O$ (35% Na_2S) in 50 ml of water is added dropwise with stirring at 0°C over a period of 2 h. After further stirring at room temp. for 30 min, the fine yellowish green product is filtered with suction, washed with water and methanol and dried. Recrystallization from toluene yields 12.3 g (75%) of **6** (*syn/anti*) as olive-colored needles. – M.p. >230°C (dec.). – IR (KBr): $\tilde{\nu} = 3050$ cm^{-1}, 2980, 2930, 2860 (C–H), 1655 (C=O), 1525 (C=C).

Thermolysis of 11.0 g (26.9 mmol) of **6** in a sublimation apparatus in portions of 1–2 g at 200–210°C/0.01 Torr yields 4.13 g (55%) of **2a** as deeply violet shining needles, m.p. 266°C (dec.). – IR (KBr): $\tilde{\nu} = 3060$ cm^{-1} (C–H), 1650, 1640 (C=O), 1530 (C=C), 1290, 1260, 1095, 1040, 880, 840, 690. – UV (CH_3CN): λ_{max} (lg ε) = 258 nm (4.18), 508 (br, 3.13). – MS (70 eV), *m/z* (%): 276 (100) [M^+].

$C_{12}H_4O_4S_2$ (276.3) Calcd. C 52.17 H 1.46
Found C 51.90 H 1.49

Cyclovoltammetry (in Dichloromethane): EG & G-PARC-175 universal programmer, Amel-553 potentiostat. Measurements in Ar-saturated dichloromethane under Ar with a Pt-working electrode (diameter 1 mm) and W-counter electrode vs. Ag/AgCl pseudoreference, standardization with ferrocene.

Cyclovoltammetry (in Acetonitrile): Amel-568 function generator, Amel-553 potentiostat, online data registration by A/D transmitter ANA 86/3[22] on a 80386SX computer. Measurements in N_2-saturated acetonitrile under N_2 with a Pt disk electrode (diameter 3 mm) vs. Ag/AgCl pseudoreference, standardization with ferrocene.

Spectroelectrochemistry: Amel-550 potentiostat, Perkin Elmer Lambda 9 spectrophotometer, thin-layer cell (150 μm) with optical transparent ITO electrodes[23] or Au minigrid between quartz win-

Tab. 5. Crystallographic data for **2a**[c]

Empirical formula	$C_{12}H_4S_2O_4$
Crystal system[a]	orthorhombic
Space group	$Cmc2_1$
a [pm]	1840.1(11)
b [pm]	1661.8(7)
c [pm]	1401.2(8)
$\alpha = \beta = \gamma$ [°]	90
Z	16
M [g mol^{-1}]	276.2
V [10^6 pm^3]	4285(4)
ϱ_{calc} [g cm^{-1}]	1.713
ϱ_{det} [g cm^{-1}]	1.69
μ [cm^{-1}]	4.32
Scan range [°]	$4.5 < 2\theta < 45$
Independent reflections[b]	1970
Reflections with $\lvert F_o\rvert \geq 3\sigma(\lvert F_o\rvert)$	1657
R	0.036
R_w	0.036

[a] Crystal size 2.0 × 0.3 × 0.1 mm^3. – [b] 2249 measured reflections in scan range $0 < h < 20$, $0 < k < 17$, $0 < l < 15$, scan width 1° (ω scan), minimal scan speed 4°/min, empirical absorption correction (ψ scan). – [c] Further details of the crystal structure analysis are available on request from the Fachinformationszentrum Karlsruhe, Gesellschaft für wissenschaftlich-technische Information mbH, W-7514 Eggenstein-Leopoldshafen 2, on quoting the depository number CSD-56805, the names of the authors and the journal citation.

dows, measurements in the range of 320–2500 nm (ITO) or 200–3200 nm (Au minigrid, quartz).

Crystal Structure Determination of **2a**: Suitable crystals for structure determination were obtained by crystallization of **2a** from chlorobenzene. The reflections were collected on a syntex $P2_1$ diffractometer by using Mo-K_α radiation (λ = 0.71069 Å, graphite monochromator). Cell constants were obtained from 15 independent reflections (Table 5).

Table 6. Fractional coordinates and equivalent isotropic thermal parameters for the asymmetrical unit of **2a**

	x/a	y/b	z/c	U_{eq}
Atom		Molecule **2a**		
C1	771(3)	5934(4)	1321(5)	31(4)
C2	368(4)	6523(4)	1900(6)	42(7)
C7	361(5)	2452(5)	-852(6)	48(8)
C8	774(4)	3162(4)	-536(6)	42(7)
C11	368(3)	5260(3)	870(5)	28(6)
C14	367(4)	3841(4)	-94(5)	32(6)
S9	964(1)	4573(1)	341(3)	40(2)
O15	3579(2)	-1002(3)	6193(5)	45(5)
O18	1429(3)	3208(4)	-633(6)	64(7)
Atom		Molecule **2a'**		
C1	3563(3)	6153(4)	6568(6)	36(7)
C2	2881(3)	5797(4)	6200(7)	44(8)
C3	2889(3)	5094(5)	5749(7)	45(8)
C4	3564(3)	4660(4)	5572(5)	30(6)
C11	4260(3)	5748(3)	6314(5)	28(6)
C12	4262(3)	5059(4)	5836(5)	26(5)
S9	5000(0)	6301(1)	6766(3)	38(2)
S10	5000(0)	4452(1)	5480(3)	29(2)
O15	3562(2)	6746(3)	7070(5)	50(6)
O16	3577(2)	3987(3)	5234(5)	43(5)
Atom		Molecule **2a''**		
C1	3559(4)	4198(4)	8065(6)	37(7)
C2	2882(4)	3810(5)	7762(7)	48(8)
C3	2875(4)	3137(5)	7255(7)	45(8)
C4	3561(4)	2751(4)	6997(6)	35(7)
C11	4259(3)	3805(4)	7793(6)	29(6)
C12	4258(3)	3134(4)	7279(5)	28(6)
S9	5000(0)	4370(2)	8224(3)	36(2)
S10	5000(0)	2554(1)	6876(3)	31(2)
O15	3567(3)	4825(3)	8503(5)	56(6)
O16	3568(3)	2115(3)	6567(5)	54(6)
Atom		Molecule **2a'''**		
C1	3563(4)	2229(4)	9437(6)	37(7)
C2	2887(4)	1810(5)	9187(7)	49(9)
C3	2884(4)	1144(5)	8698(7)	51(9)
C4	3563(4)	769(5)	8374(6)	41(7)
C11	4263(3)	1841(4)	9145(5)	29(6)
C12	4262(3)	1160(4)	8638(6)	30(6)
S9	5000(0)	2421(1)	9546(3)	35(2)
S10	5000(0)	599(2)	8205(0)	41(3)
O15	3575(3)	2866(3)	9847(5)	56(6)
O16	3569(3)	162(4)	7888(6)	60(7)

Automated Patterson-solving techniques (SHELX-86[13a]) were generally unsuccessful in solving the structure in space groups $Cmc2_1$, *Ama*2, and *Cmcm*, as were Patterson rotation-translation search methods (PATSEE)[13b]. Initial attempts to apply direct methods (DIRDIF, MULTAN-80, SIR)[13c–e] were also unfruitful. The structure was finally solved by using the direct methods option ("TREF 2000") of SHELX-86 in space group $Cmc2_1$, which revealed the positions of three of the four TDQ fragments. These three fragments are all bisected by mirror planes. Refinement of these atomic positions (using SHELX-76[13f], full-matrix least-squares) then revealed the fourth dithiine molecule of the asymmetric unit (Table 6).

The positions of the hydrogen atoms were obtained by difference Fourier analysis and refined isotropically at a fixed carbon hydrogen bond length of 0.92 Å.

[1] LIX. Mitteilung: E. Günther, S. Hünig, J.-U. von Schütz, U. Langohr, H. Rieder, S. Söderholm, H.-P. Werner, K. Peters, H. G. von Schnering, H. J. Lindner, *Chem. Ber.* **1992**, *125*, 1919–1926.

[2] [2a] H. Bock, A. Rauschenbach, K. Ruppert, Z. Havlas, *Angew. Chem.* **1991**, *103*, 706–708; *Angew. Chem. Int. Ed. Engl.* **1991**, *30*, 714. – [2b] H. Bock, D. Jaculi, *Z. Naturforsch.*, Teil B, im Druck.

[3] [3a] T. Weiß, G. Klar, *Liebigs Ann. Chem.* **1978**, 785–788. – [3b] P. Berges, G. Klar, *Z. Naturforsch., Teil B*, **1988**, *43*, 599–604.

[4] D. O. Cowan, A. Kini, L. Chiang, K. Lerstrup, D. R. Talham, T. O. Poehler, A. N. Bloch, *Mol. Cryst. Liq. Cryst.* **1982**, *86*, 1–26.

[5] W. Hinrichs, H.-J. Riedel, G. Klar, *J. Chem. Res. (S)* **1982**, 334–335.

[6] W. Hinrichs, P. Berges, G. Klar, *Z. Naturforsch., Teil B*, **1987**, *42*, 169–176.

[7] [7a] A. Aumüller, S. Hünig, *Liebigs Ann. Chem.* **1986**, 142–164. – [7b] A. Aumüller, P. Erk, S. Hünig, H. Meixner, J.-U. von Schütz, H.-P. Werner, *Liebigs Ann. Chem.* **1987**, 997–1006.

[8] E. S. Martinez, R. D. Calleja, J. Behrens, P. Berges, J. Kudnig, N. Wölki, G. Klar, *J. Chem. Res. (S)* **1991**, 246–247.

[9] K. Fickentscher, *Chem. Ber.* **1969**, *102*, 1739–1742.

[10] K. Brass, L. Köhler, *Ber. Dtsch. Chem. Ges.* **1922**, *55*, 2543.

[11] B. Wladislaw, L. Marzorati, C. Di Vitta, *Synthesis* **1983**, 464–466.

[12] H. Rakoff, B. H. Miles, *J. Org. Chem.* **1961**, *26*, 2581–2584.

[13] [13a] G. M. Sheldrick, *SHELX-86, Program for Crystal Structure Determination*, University of Cambridge, **1986**. – [13b] E. Egert, G. M. Sheldrick, *PATSEE (Fragment Search by Integrated Patterson and Direct Methods)*, *Acta Crystallogr., Sect. A*, **1985**, *41*, 262–268. – [13c] P. T. Beurskens, H. P. Bosmans, H. M. Doesburg, R. O. Gould, T. E. van der Hark, P. A. J. Prick, J. H. Noordik, G. Beurskens, V. Parthasarathi, *DIRDIF (Direct Methods for Difference Structures)*, University of Nijmegen (The Netherlands). – [13d] G. Germain, P. Main, M. M. Woolfson, *MULTAN-80*, University of Luovain (Belgium), **1980**. – [13e] M. C. Burla, M. Camalli, G. Cascaranco, C. Giacovazzo, G. Polidori, R. Spagna, D. Viterbo, *Program SIR-88*, University of Bari (Italy), **1988**. – [13f] G. M. Sheldrick, *SHELX-76, Program for Crystal Structure Determination*, University of Cambridge, **1976**.

[14] J. J. P. Stewart, F. J. Seiler, *MOPAC 6.0*, *QCPE-Programm Nr. 455*. Calculations were carried out without assumptions regarding structure or symmetry, respectively, with exception of **1b** and $\mathbf{1b}^{\bullet+}$, which were calculated on the assumption of methoxy groups aligned parallel to the plane of the aromatic ring.

[15] *PCMODEL, Molecular Modeling software for the IBM/XT/AT*, **1987**, Serena Software, BOX 3076, Bloomington, Indiana 47402, USA.

[16] I. Rowe, B. Post, *Acta Crystallogr.* **1958**, *11*, 372–374.

[17] P. Berges, W. Hinrichs, K.-W. Stender, G. Klar, *J. Chem. Res. (S)* **1987**, 326–327.

[18] W. A. Dollase, *J. Am. Chem. Soc.* **1965**, *87*, 979–982.

[19] [19a] T. H. Jozefiak, J. E. Almlöf, M. W. Feyereisen, L. L. Miller, *J. Am. Chem. Soc.* **1989**, *111*, 4105–4106. – [19b] J. E. Almlöf, M. W. Feyereisen, T. H. Jozefiak, L. L. Miller, *J. Am. Chem. Soc.* **1990**, *112*, 1206–1214.

[20] G. A. Russell, N. K. Suleman, H. Iwamura, O. W. Webster, *J. Am. Chem. Soc.* **1981**, *103*, 1560–1561.

[21] N. S. Hush, *Coord. Chem. Rev.* **1985**, *64*, 135; K. W. Penfield, J. R. Miller, M. N. Paddon-Row, E. Cotsaris, A. M. Oliver, N. S. Hush, *J. Am. Chem. Soc.* **1987**, *109*, 5061–5065.

[22] A/D transmitter ANA 86/3, developed by Rechenzentrum Universität Regensburg.

[23] J. Salbeck, I. Aurbach, J. Daub, *Dechema Monographien* **1988**, *112*, 177.

[286/92]